Stem Cell Reports
Report

ISSCR

OPEN ACCESS

Spindle Misorientation of Cerebral and Cerebellar Progenitors Is a Mechanistic Cause of Megalencephaly

Huaibiao Li,[1] Torsten Kroll,[1] Jürgen Moll,[2] Lucien Frappart,[1,3] Peter Herrlich,[1] Heike Heuer,[1,4] and Aspasia Ploubidou[1,*]

[1]Leibniz Institute on Aging, Fritz Lipmann Institute, 07745 Jena, Germany
[2]Boehringer-Ingelheim RCV & Co KG, 1121 Vienna, Austria
[3]INSERM, Oncogenèse et Progression Tumorale, Université Claude Bernard Lyon I, 69373 Lyon, France
[4]Present address: Leibniz Research Institute for Environmental Medicine, 40225 Düsseldorf, Germany
*Correspondence: aspasia.ploubidou@leibniz-fli.de
http://dx.doi.org/10.1016/j.stemcr.2017.08.013

SUMMARY

Misoriented division of neuroprogenitors, by loss-of-function studies of centrosome or spindle components, has been linked to the developmental brain defects microcephaly and lissencephaly. As these approaches also affect centrosome biogenesis, spindle assembly, or cell-cycle progression, the resulting pathologies cannot be attributed solely to spindle misorientation. To address this issue, we employed a truncation of the spindle-orienting protein RHAMM. This truncation of the RHAMM centrosome-targeting domain does not have an impact on centrosome biogenesis or on spindle assembly *in vivo*. The RHAMM mutants exhibit misorientation of the division plane of neuroprogenitors, without affecting the division rate of these cells, resulting against expectation in megalencephaly associated with cerebral cortex thickening, cerebellum enlargement, and premature cerebellum differentiation. We conclude that RHAMM associates with the spindle of neuroprogenitor cells via its centrosome-targeting domain, where it regulates differentiation in the developing brain by orienting the spindle.

INTRODUCTION

Proliferative and neurogenic divisions of neuroprogenitor cells are spatially orchestrated. The former exhibit planar (i.e., occurring in the epithelial plane) and the latter generally apicobasal orientation, although neurogenic divisions may proceed through several intermediate steps (Peyre and Morin, 2012). Orientation of neuroprogenitor divisions may therefore be causal to cell fate.

The division plane of neuroprogenitors is determined by the mitotic spindle, on which extracellular and intracellular cues converge to modulate its positioning. It is well established that cortical cues and molecular motors, such as NuMA-LGN-dynein, signal to the mitotic spindle ensuring its proper orientation (Kotak et al., 2012). Perturbation of these cortical signals (e.g., by LGN truncation or modulation of Inscruteable expression) alters the orientation of the neuroprogenitor division plane and, consequently, cell fate of daughter cells, supporting that orientation of neuroprogenitor divisions is the key cell-fate determinant of neuroprogenitors (Konno et al., 2008; Postiglione et al., 2011; Falk et al., 2017). Nevertheless, the spindle mechanism detecting cell extrinsic or intrinsic cues and translating them to orientation of the division plane, thus regulating spindle response to cortical cues, is largely unknown.

Loss of function of centrosomal or spindle components in animal models perturbs spindle orientation in cortical neuroprogenitors, linking these defects to microcephaly and lissencephaly (Sun and Henver, 2014; Fish et al., 2006; Gruber et al., 2011; Fujimori et al., 2013; Chen et al., 2014). These animal model studies corroborate the previously reported association of human microcephaly with mutations in centrosomal proteins (Jackson et al., 2002; Bond et al., 2002, 2005; Guernsey et al., 2010).

However, loss of function of centrosomal or spindle components also affects centrosome biogenesis, cell-cycle progression, and spindle assembly. This has raised the question whether microcephaly is driven by defects in spindle assembly or orientation (Noatynska et al., 2012; Peyre and Morin, 2012) and the need for more specific approaches to address the impact of spindle (mis)orientation on brain development, e.g., by employing a "pure" spindle misorientation model (Noatynska et al., 2012).

A suitable candidate for such an approach is RHAMM.

RHAMM is a spindle-associated protein (Assmann et al., 1999) upregulated during the cell cycle in G2/M (Sohr and Engeland, 2008). It is required for spindle integrity *in vitro* (Maxwell et al., 2003; Groen et al., 2004; Joukov et al., 2006) and for spindle orientation *in vitro* (Dunsch et al., 2012) and *in vivo* (Li et al., 2015, 2016). Importantly, depletion (Neumann et al., 2010) or *in vivo* truncation (Li et al., 2015, 2016) of the RHAMM centrosome-targeting domain does not block bipolar spindle assembly. RHAMM mRNA is expressed in proliferating regions of the larval *Xenopus* brain, suggesting a brain developmental function (Casini et al., 2010).

RESULTS AND DISCUSSION

RHAMM mRNA is highly expressed in the proliferative areas of the embryonic (Figure 1A) and postnatal (Figure 1B)

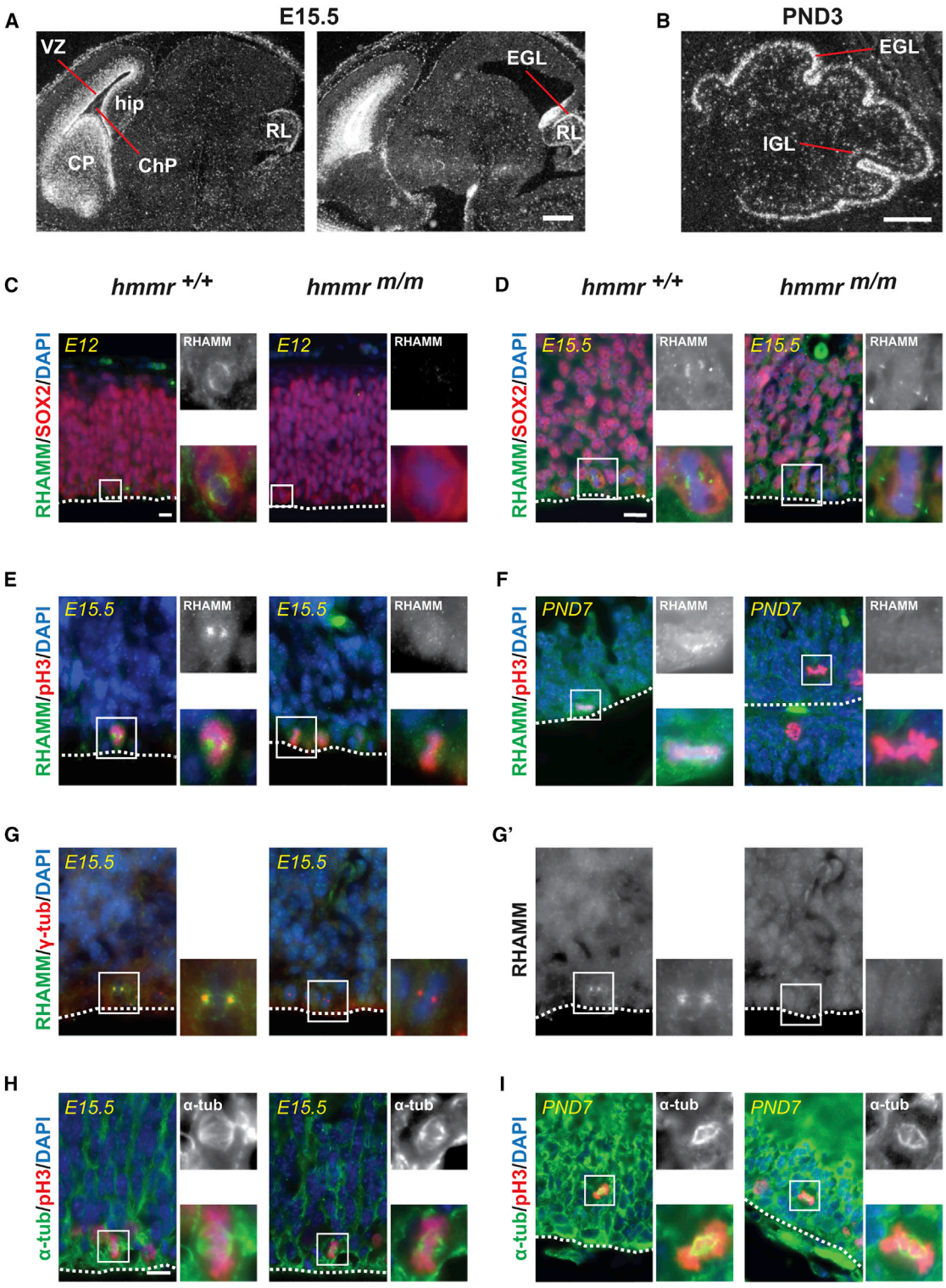

Figure 1. RHAMM Expression and Localization in Embryonic and Neonatal Mouse Brain

(A and B) Embryonic E15.5 (A) and neonatal PND3 (B) brain sections subjected to *in situ* hybridization, reveal RHAMM mRNA expression in forebrain and cerebellum. ChP, choroid plexus; CP, caudate putamen; hip, hippocampus; RL, rhombic lip; VZ, ventricular zone.

(legend continued on next page)

mouse brain, in particular at the ventricular zone (VZ) of the cerebral cortex and at the external granule layer (EGL) of the cerebellar cortex, where progenitor or precursor cells divide before differentiating to neurons.

The protein localizes at the spindle of human and mouse cells via the RHAMM centrosome-targeting domain (Assmann et al., 1999; Maxwell et al., 2003; Li et al., 2015). To analyze the mitotic function of RHAMM in the brain, we employed the *hmmr*$^{m/m}$ mouse model, which expresses truncated RHAMM lacking the centrosome-targeting domain (Li et al., 2015). During development of wild-type *hmmr*$^{+/+}$ brain, RHAMM localized at the spindle of the mitotic cells of the cerebral and cerebellar cortex (Figures 1 and S1A), including SOX2-expressing apical neuroprogenitors of the cerebrum (Figures 1C and 1D) and the EGL cells of the cerebellum (Figures 1B and 1F).

This localization is abolished in the mutant *hmmr*$^{m/m}$ mouse (Figures 1 and S1A). RHAMM dissociation from the mitotic apparatus (Figures 1C–1G′) did not impair bipolar spindle assembly in the brain (Figures 1H and 1I), supporting the notion that the C terminus is dispensable for spindle assembly *in vivo* (Li et al., 2015, 2016). Although RHAMM is essential for acentrosomal spindle integrity (Groen et al., 2004; Joukov et al., 2006), it appears dispensable for centrosomal spindle formation and cell-cycle progression, as indicated by antibody (Maxwell et al., 2003), siRNA (Figure S1B; Neumann et al., 2010; Dunsch et al., 2012; Li et al., 2016), or genetically mediated disruption, including *in vivo* studies of mouse and human (Tolg et al., 2003; Li et al., 2015, 2016).

RHAMM regulates, however, spindle orientation (Figure 2) in the two brain cell types that perform oriented division (Sun and Hevner, 2014; Zagon and McLaughlin, 1987).

Determination of the median θ angle between the spindle axis and the apical plane (Figure 2A) revealed that apical neuroprogenitors in the cerebral cortex of *hmmr*$^{+/+}$ mice undergo predominantly planar division. This is demonstrated by the division plane angle θ of 8.2° (E15.5 [embryonic day 15.5], metaphase; Figure 2B) and 8.3° (E15.5, anaphase; Figure 2C), in agreement with previous studies (Noctor et al., 2008; Konno et al., 2008; Xie et al., 2013; Falk et al., 2017). In *hmmr*$^{m/m}$ progenitors, median θ increased to 16.2° (E15.5, metaphase) and 23.3° (E15.5, anaphase), indicative of significantly elevated apicobasal divisions (Figures 2B–2D). This elevation was already detectable and significant at E12 (median θ of 22.1° in *hmmr*$^{m/m}$ versus 9.8° in wild-type control brain) (Figure 2D).

Metaphase spindles rotate within the general plane of division, which is determined by upstream components (e.g., NuMA-LGN-dynein), before reaching their final orientation at anaphase (Adams, 1996; Siller and Doe, 2009; Peyre and Morin, 2012). Indeed, the majority of *hmmr*$^{+/+}$ apical neuroprogenitors exhibit planar orientation at both phases. In *hmmr*$^{m/m}$ E12 as well as E15.5 progenitors, the percent of planar divisions is further decreased at anaphase, compared with metaphase, suggesting that the upstream mechanisms cannot sustain the preferred (planar) orientation in the absence of RHAMM-spindle interaction. This finding is consistent with the notion that spindle components (including RHAMM) act as sensors and enforcers of cell intrinsic/extrinsic cues in orienting the division plane (di Pietro et al., 2016).

There are conflicting reports on the orientation of the division plane of postnatal granule cell precursors (GCP) in the cerebellar EGL (Zagon and McLaughlin, 1987; Williams et al., 2015; Haldipur et al., 2015). We found that, prior to establishing the direction of division, the spindle of GCPs undergoes random orientation (Figures S1C– S1E). At anaphase, GCPs adjacent to the pial surface displayed preferential apicobasal division (Figures 2F and 2G). The percentage of GCPs undergoing planar division further decreased in *hmmr*$^{m/m}$ (Figures 2G and 2H), suggesting a shift from planar to apicobasal divisions caused by RHAMM dysfunction.

RHAMM orients the spindle via interaction with CHICA and DYNLL1 (Dunsch et al., 2012). The *hmmr*$^{m/m}$-encoded truncated protein (RHAMM-ΔC) cannot interact with DYNLL1 (Figure 2I) or with CHICA (Li et al., 2016), suggesting that it is the disruption of the RHAMM-DYNLL1 interaction in the *hmmr*$^{m/m}$ brain that impairs oriented division of cerebral and cerebellar progenitors.

Collectively, the above data indicate that the centrosome-targeting domain of RHAMM is not essential for bipolar spindle assembly *in vivo*, but it is indispensable for regulated planar division of cerebral neuroprogenitors and GCPs.

What is the consequence of this deregulation for brain development?

In the cerebellum, the GCPs, similarly to cerebral progenitors, detach from the pial surface before they start to differentiate (Butts et al., 2014). Thus, an elevated number of apicobasal divisions would be expected to lead to premature

(C–I) Immunofluorescence localization of RHAMM at the spindle and centrosome of ventricular zone cerebral neuroprogenitors at E12 (C) and E15.5 (D, E, G, and G′) and of cerebellar EGL cells at PND7 (F) in *hmmr*$^{+/+}$ but not *hmmr*$^{m/m}$ brain. Neither cerebral (H) nor cerebellar (I) *hmmr*$^{m/m}$ cells present obvious spindle defects. The apical cerebral cortex (C–E, G, G′, and H) and the pial cerebellar (F and I) surface are indicated by the dotted lines.
Scale bars: 500 μm (A and B), 10 μm (C–I).

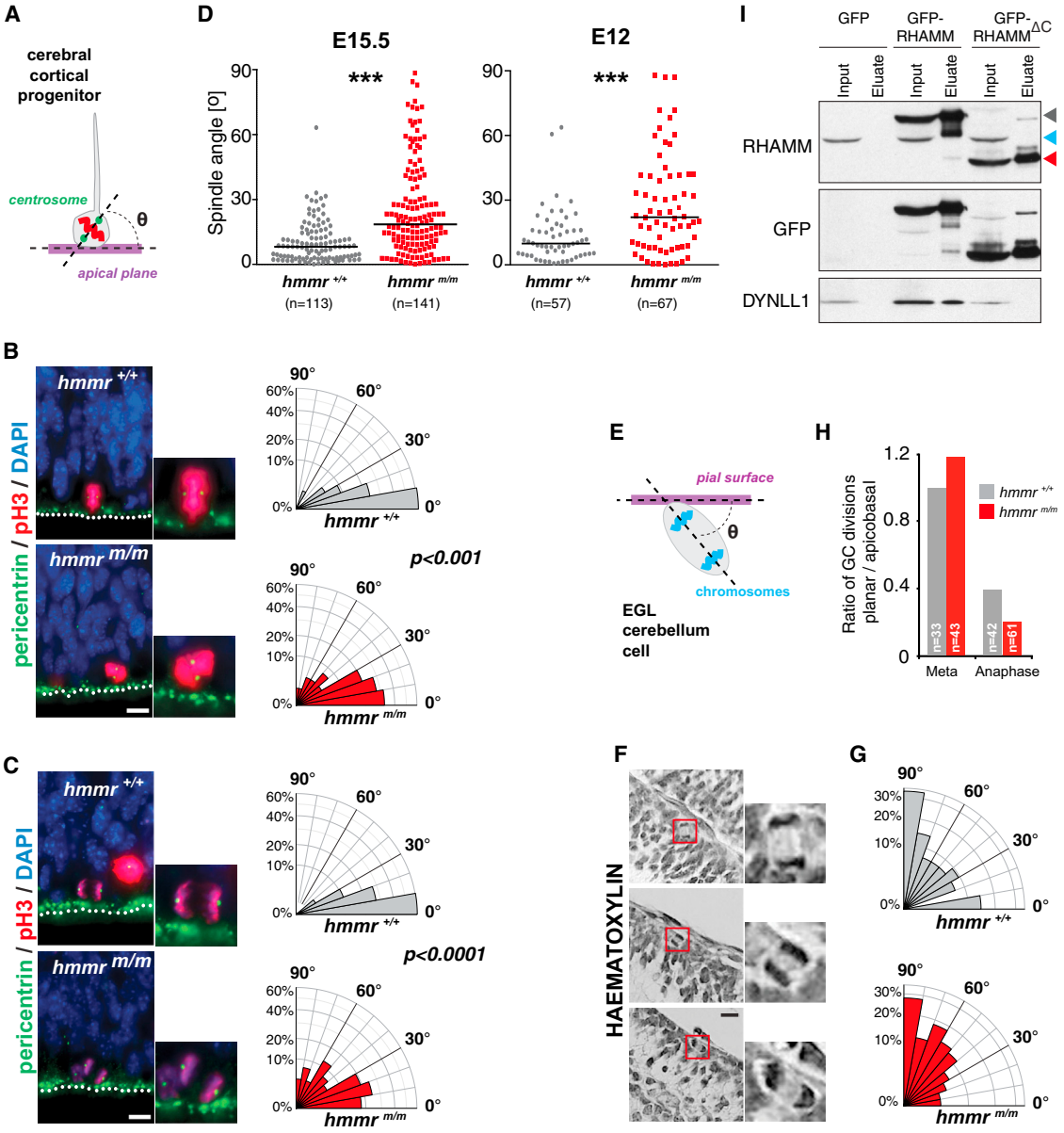

Figure 2. RHAMM Regulates Spindle Orientation of Neuroprogenitors in Cerebrum and Cerebellum, via Its Centrosome and Dynein-Binding Domain

Embryonic E15.5 (B and C) or E12 and neonatal PND7 (F) brain sections used in quantification of division angle θ of cerebral cortex apical neuroprogenitors (A–D) or cerebellar EGL cells (E–H). Scale bar: 10 μm. ***p < 0.001; n = number of cells analyzed. Orientation histograms (B, C, and G) indicate θ. Detailed description in Experimental Procedures. RHAMM C terminus truncation prevents association with DYNLL1 (I), demonstrated by immunoprecipitation. Arrowheads: endogenous RHAMM (blue), GFP-RHAMM (gray), GFP-RHAMM-ΔC (red).

differentiation of GCPs. Indeed, at PND7 (postnatal day 7), the *hmmr*$^{m/m}$ cerebellum is larger in size and displays advanced differentiation (Figure 3A), demonstrated by increased thickness of the molecular layer (ML) and decreased thickness of the EGL (Figure 3B).

The rate of division of GCPs remains the same between wild-type and mutant (Figures 3C and 3D), suggesting that RHAMM regulates the differentiation of GCPs in the cerebellum. This conclusion is supported by the accelerated disappearance of EGL in the mutant (Figures 3E and 3F), consistent with the premature increase in PAX6-positive GCs in the IGL (Figures 3E and 3G). There is no significant change in the number of Purkinje cells (Figure 3H), which are of different lineage from the CGPs.

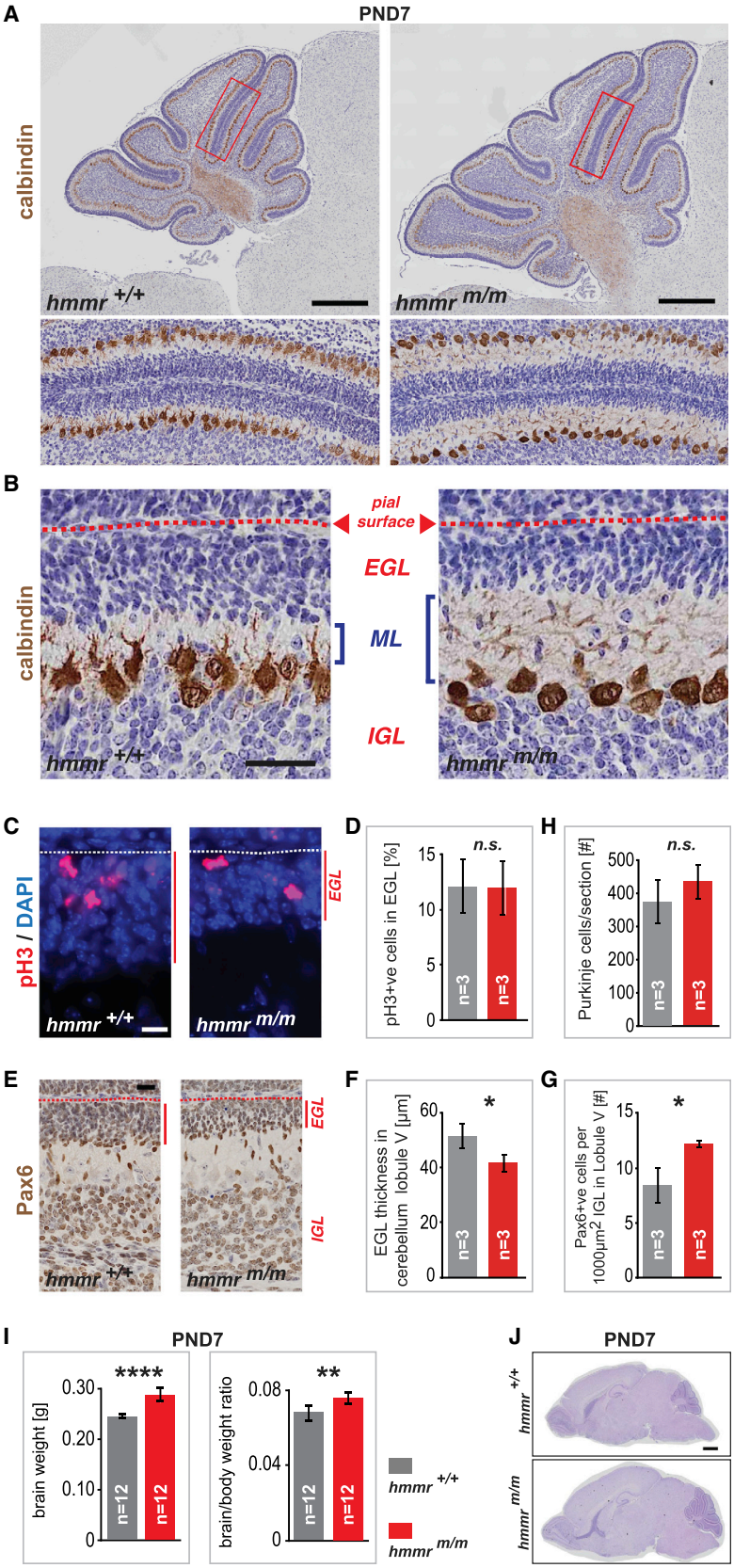

Figure 3. The RHAMM Centrosome-Targeting Domain Is Required for Normal Cerebellum Development

(A–H) Enlargement (A) and accelerated cerebellum differentiation in *hmmr*$^{m/m}$ at PND7 indicated by advanced dendritogenesis of calbindin-labeled Purkinje cells (ML) (A and B), reduction of EGL thickness (B, C, E, and F), and increase in PAX6-expressing cells localized in the IGL (E and G).The rate of cell division is not altered in the expanded EGL of the mutant (C and D), neither is the number of Purkinje cells (A, B, and H).

(I and J) Brain enlargement of *hmmr*$^{m/m}$ at PND7 (J) quantified by brain weight normalized to body weight (I).

Scale bars: 200 µm (A), 20 µm (B and E), 10 µm (C), 1 mm (J). *p < 0.05; **p < 0.01, ****p < 0.0001; n = number of animals analyzed; for further statistical information see Experimental Procedures.

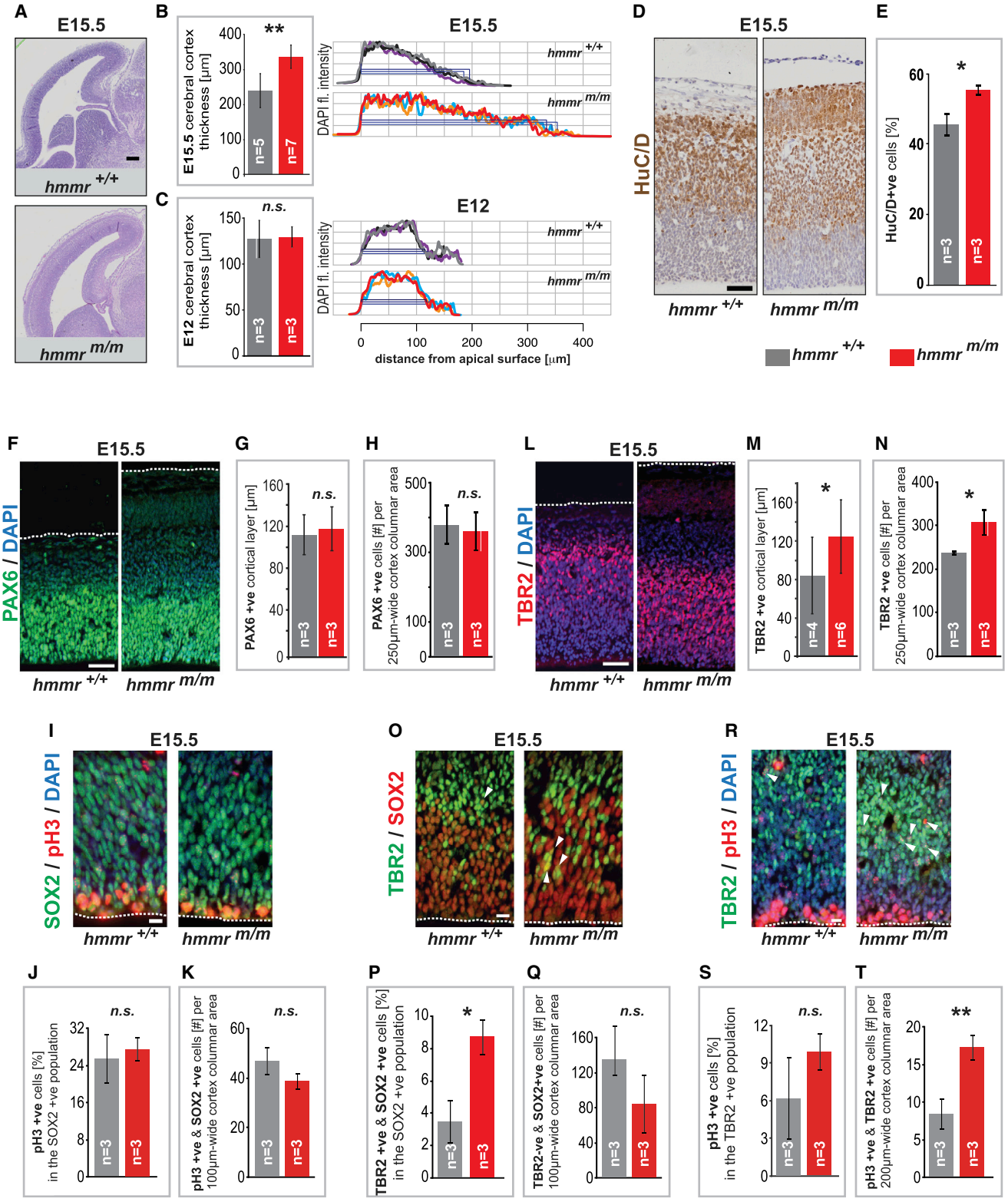

Figure 4. The RHAMM Centrosome-Targeting Domain Is Required for Normal Cerebral Cortex Development

(A–E) Cerebrum enlargement of embryonic *hmmr*$^{m/m}$ brain is detectable from E15.5 (but not at E12, C) demonstrated by increased cortical wall thickness (A and B) and increased neurogenesis (D and E).

(legend continued on next page)

The strong *hmmr*$^{m/m}$ cerebellar phenotype (Figure 3A), consistent with a shift from planar to apicobasal GCP divisions, is poorly reflected in the modest spindle orientation defect of GCPs (Figure 2G). These data suggest the existence of distinct GCP subpopulations in the EGL, each having a different preferred division plane orientation (similarly to basal germ cell subpopulations; Li et al., 2016). We were not able to test this hypothesis, as GCP subpopulation markers have not yet been identified.

Consistent with the premature cerebellum differentiation and enlargement at PND7, the *hmmr*$^{m/m}$ animals present with megalencephaly (Figures 3I and 3J). This pathology is already detectable during embryogenesis when cerebrum development is affected (Figure 4A). Compared with *hmmr*$^{+/+}$ controls, the mutants develop a thick cerebral cortical wall, detectable from E15.5 but not at E12 (cf. Figures 4B and 4C). Accordingly, the *hmmr*$^{m/m}$ brain exhibits increased generation of differentiating neurons, demonstrated by HuC/HuD labeling (Figures 4D and 4E).

Cerebral neurons are derived from apical progenitors (APs) via proliferative and neurogenic divisions (the former exhibiting planar and the latter generally apicobasal orientation). The neurogenic apicobasal divisions generate intermediate progenitors (IPs) and give rise to differentiated neurons. Given the very significant increase in apicobasal divisions in *hmmr*$^{m/m}$ (Figure 2D), we analyzed the impact of truncation on the AP and IP populations expressing PAX6/SOX2 and TBR2, respectively (Woodworth et al., 2012).

At E12, when neurogenesis begins, the RHAMM truncation significantly impaired the spindle orientation of AP cells (Figure 2D) but had no effect on the division rate of either AP (Figures S2A–S2C) or IP cells (Figures S2D–S2F) or on cerebral cortex thickness (Figure 4C). At E15.5, the PAX6/SOX2-expressing AP layer was unaffected by the mutation, as demonstrated by layer thickness (Figures 4F, 4G, and S2G), number of APs (Figure 4H), and their rate of proliferation (Figures 4I–4K), compared with wild-type *hmmr*$^{+/+}$ APs. In contrast, the number of TBR2-expressing IPs and the thickness of the TBR2-positive subventricular layer were significantly increased in the *hmmr*$^{m/m}$ cortex (Figures 4L–4N and S2H). Thus, spindle misorientation precedes cortical enlargement in *hmmr*$^{m/m}$, suggesting that randomization of the AP cell division plane is causative of the cerebrum developmental defect.

As TBR2-positive cells are derived from the apicobasal division of APs, we hypothesized that the excessive apicobasal division of APs in *hmmr*$^{m/m}$ causes a change in cell fate of the daughter cells, contributing to the expanded TBR2-expressing cell layer. We thus analyzed the relative abundance of progenitors expressing both SOX2 and TBR2, because they are thought to represent IPs newly derived from APs (Englund et al., 2005). These cells were significantly increased in *hmmr*$^{m/m}$ (Figures 4O and 4P), consistent with a decrease, per unit area of the cortex, in the cells that express SOX2 but not TBR2 (Figure 4Q).

These data suggest that increased generation of IPs contributes to the expanded TBR2-expressing layer (Figures 4M and 4N). Indeed, the mutant brain has a higher number of dividing TBR2-positive cells than wild-type (Figures 4R and 4T). Notably, although the total cell population of TBR2+ progenitors increases, the rate of division of IPs remains unaltered in the mutant (Figures 4R and 4S), supporting the notion that the RHAMM truncation has no adverse effects on spindle assembly or cell-cycle progression. This conclusion is further supported by the finding that the *hmmr*$^{m/m}$ cerebral cortex exhibits no increase in apoptosis (Figure S2I), differing from previous models in which centrosome biogenesis or spindle assembly are disrupted, resulting in elevated apoptosis (Yingli et al., 2008; Gruber et al., 2011; Insolera et al., 2014).

Taken together, these data indicate that the misoriented (apicobasal) divisions of PAX6/SOX2-expressing APs led to an increased number of replicating TBR2-expressing IPs in *hmmr*$^{m/m}$ (Figures 4R and 4T), contributing to cerebral cortex enlargement and megalencephaly. Hence, RHAMM regulates the cell fate of neuronal progenitors by orienting their spindle.

The accelerated differentiation in the *hmmr*$^{m/m}$ brain does not have long-lasting impact on brain size. After completion of the neuronal differentiation period, the cerebellum and cerebrum of the mutants have similar size to their wild-type counterparts (Figures S1F, S1G, and S2J).

In summary, the brain enlargement and absence of microcephaly in *hmmr*$^{m/m}$ indicate that spindle orientation defects alone are not sufficient to cause microcephaly. This conclusion is supported by centriole ablation in the cortex that misorients the spindle and induces microcephaly; the

(F–T) Analysis of apical (F–H) and intermediate (L–N) neuroprogenitor cells demonstrates increase of the latter in *hmmr*$^{m/m}$, quantified using cerebral cortical layer thickness (G and M) and cell number (H and N) indicators. The rate of division of E15.5 apical (J) and intermediate (S) neuroprogenitors is not altered in the mutant, but the absolute number of dividing intermediate cells is significantly increased (T), in agreement with the increase in the number of SOX2 and TBR2 double-positive progenitors (P). The number of dividing apical progenitors (K) and of SOX2-positive TBR2-negative cells (Q) remains unaltered in the mutant. Dotted line indicates the basal (F and L) or the apical (I, O, and R) surface of the cerebral cortex. Arrowheads indicate double-positive cells (O and R).
Scale bars: 200 μm (A), 50 μm (D, F, and L), 10 μm (I, O, and R). *p < 0.05, **p < 0.01; n = number of animals analyzed; for further statistical information, see Experimental Procedures.

latter can be rescued by deletion of p53 without correcting spindle misorientation (Insolera et al., 2014).

Our results suggest that spindle misorientation of APs randomizes their predominantly planar divisions (Noctor et al., 2008; Konno et al., 2008; Postiglione et al., 2011; Xie et al., 2013; Falk et al., 2017), resulting in increased generation of IPs. Thus, the *hmmr*$^{m/m}$ mouse provides support to the indirect neurogenesis model, which postulates that IPs are formed via apicobasal division, thereby amplifying neuron generation (Postiglione et al., 2011; Konno et al., 2008).

EXPERIMENTAL PROCEDURES

Mouse transgenesis has been described previously (Li et al., 2015). Colony maintenance and breeding were performed in accordance with the regulations of the relevant authority (TLV, Thüringen, Germany) and under the oversight of the FLI Animal Welfare Committee.

Orientation of Neuroprogenitor Cell Division and Statistical Analysis

The brain sections were labeled with anti-pH3 and -pericentrin/γ-tubulin antibodies to visualize mitotic chromosomes and centrosomes, respectively. Mitotic cells (neuroprogenitors adjacent to the apical membrane of the ventricular side of the cerebral cortex [Figures 2A–2C] or GCPs adjacent to the pial surface of the cerebellum [Figures S1B and S1C]) were identified as pH3-positive cells. Images were acquired with an Axiovert 200 microscope (Zeiss) with a 63× objective and imported in ImageJ (NIH). From the images, the long spindle axis of these cells, defined as a line across the two centrosomes, was used to indicate the cell division plane (Figures 2A and S1C). The apical plane of the cortex (or the pial plane of the cerebellum), adjacent to the mitotic neuroprogenitor, was defined by a line parallel to the membrane passing the membrane/cell contact point (Figures 2A and S1C). For each neuroprogenitor (or EGL precursor cell), the angle θ between the long spindle axis and the cortex apical (or cerebellum pial) plane was measured in ImageJ.

Alternatively, images of H&E-stained brain sections were imported in ImageJ. Anaphase EGL precursor cells were identified according to their chromosome status. Only the anaphase cells in layer 1, adjacent to the pial surface, were used in the quantification (Zagon and McLaughlin, 1987). The long spindle axis of these cells, defined as a line dissecting both sets of separating chromosomes, was used to indicate the cell division plane (Figure 2E). The spindle axis was defined as the line parallel to the direction of separating chromosomes. Adjacent to the mitotic cell, the pial plane of the cerebellum was defined by a line parallel to the membrane passing the cell/membrane contact point (Figure 2E). For each EGL precursor cell, the angle θ between the long spindle axis and the cerebellum pial plane was measured in ImageJ.

The neocortex of three *hmmr*$^{+/+}$ and four *hmmr*$^{m/m}$ E15.5 embryos, three *hmmr*$^{+/+}$ and three *hmmr*$^{m/m}$ E12 embryos, or the cerebellum of four *hmmr*$^{+/+}$ and four *hmmr*$^{m/m}$ 7-day old (PND7) neonates were used in the analysis. The difference in θ between wild-type and mutants was analyzed via the Wilcoxon rank-sum test with continuity correction.

For cortical neuroprogenitors of E15.5 embryos, the difference in θ between *hmmr*$^{+/+}$ and *hmmr*$^{m/m}$ at metaphase was 6.9° with a 95% confidence interval of 3.0°–10.8°, p = 0.000268 (*hmmr*$^{+/+}$, n = 65; *hmmr*$^{m/m}$, n = 84) (Figure 2B). At anaphase, the difference in the two populations in θ increased to 15.6° with a 95% confidence interval of 10.7°–23.8°, $p = 4.316 \times 10^{-8}$ (*hmmr*$^{+/+}$, n = 48; *hmmr*$^{m/m}$, n = 57) (Figure 2C). When cells at metaphase and anaphase were pooled, the difference in θ remained highly significant (p = 3.018e-10) (Figure 2D, E15.5).

For cortical neuroprogenitors of E12 embryos, the difference of θ between *hmmr*$^{+/+}$ and *hmmr*$^{m/m}$ at metaphase was not significant (*hmmr*$^{+/+}$, n = 42; *hmmr*$^{m/m}$, n = 39; p = 0.1842) (Figure 2B). However, at anaphase, the 20.9° difference in θ between the two populations was highly significant with a 95% confidence interval of 10.6°–36.4°, $p = 2.819 \times 10^{-4}$ (*hmmr*$^{+/+}$, n = 15; *hmmr*$^{m/m}$, n = 28). When cells at metaphase and anaphase were pooled, the difference of θ remained highly significant ($p = 4.746 \times 10^{-4}$) (Figure 2D, E12).

For cerebellar EGL precursor cells, the difference in θ between *hmmr*$^{+/+}$ and *hmmr*$^{m/m}$ at both metaphase (*hmmr*$^{+/+}$, n = 33; *hmmr*$^{m/m}$, n = 43) and anaphase (*hmmr*$^{+/+}$, n = 42; *hmmr*$^{m/m}$, n = 61) was not significant (metaphase, p = 0.9124; anaphase, p = 0.9946). The ratio of planar versus perpendicular divisions was calculated as the ratio of cells with spindle angle at 0–30° compared with cells with spindle angle at 60–90° (Figure 2H).

The hypothesis that cortical neuroprogenitor spindle orientation is random was tested by the Kolmogorov-Smirnov test. The test was applied on the distribution of spindle angles against an assumed random distribution (each angle has the same probability of appearing), normalizing the angle θ between 0 and 1.

(1) of cortical neuroprogenitors at E15.5 (metaphase: D = 0.48032, $p < 2.2 \times 10^{-16}$ for *hmmr*$^{m/m}$; D = 0.63231, $p < 2.2 \times 10^{-16}$ for *hmmr*$^{+/+}$; anaphase: D = 0.2807, p = 0.0002512 for *hmmr*$^{m/m}$; D = 0.67611, $p < 2.2 \times 10^{-16}$ for *hmmr*$^{+/+}$)

(2) of cerebellar EGL precursor cells (metaphase: D = 0.10434, p = 0.6983 for *hmmr*$^{m/m}$; D = 0.10909, p = 0.8271 for *hmmr*$^{+/+}$; anaphase: D = 0.30911, $p = 1.732 \times 10^{-5}$ for *hmmr*$^{m/m}$; D = 28,571, p = 0.002104 for *hmmr*$^{+/+}$).

The test shows that the distribution of spindle angles of the wild-type and mutant cortical cells differ highly significantly from the random distribution in both metaphase and anaphase, and that the predominant (planar) spindle orientation is impaired in *hmmr*$^{m/m}$ toward a random distribution.

In contrast, the distribution of spindle angles in the wild-type and mutant cerebellar EGL precursor cells appear to be uniformly distributed with no preferred orientation, comparable with the random distribution at metaphase, but significantly differs from the random distribution at anaphase. This analysis indicates that, prior to establishing the direction of division, the spindle of these cells undergoes random orientation (Figure S1D). Subsequently, the EGL precursor cells preferentially divide apico-basally (i.e., perpendicular to the pial surface) at anaphase (Figures 2G and 2H).

Statistical Analysis

Spindle orientation was analyzed by the Wilcoxon rank-sum test and presented as an area plot or dot plot with the median

indicated. All other assays were analyzed with the two-tailed Student's t test. Those results are presented as mean ± SD. The hypothesis that neuroprogenitor spindle orientation in the cortex and cerebellum is random was tested by the Kolmogorov-Smirnov test.

Further information on methodology and materials used can be found in the Supplemental Information section.

SUPPLEMENTAL INFORMATION

Supplemental Information includes Supplemental Experimental Procedures and two figures and can be found with this article online at http://dx.doi.org/10.1016/j.stemcr.2017.08.013.

ACKNOWLEDGMENTS

The support of the Animal House, Histology, and Imaging facilities of the FLI is gratefully acknowledged, especially the expert assistance of Dominique Galendo, Jenny Buchelt, Maik Baldauf, and Linda Rothenburger. We thank Alicia Tapias Soler for discussions on brain development; Zhongwei Zhou for instruction on brain dissection; and Christopher A. Maxwell, Kerstin Feistel, and Shalmali Shukla for discussions on RHAMM function and their comments on the manuscript.

Received: June 29, 2016
Revised: August 22, 2017
Accepted: August 22, 2017
Published: September 21, 2017

REFERENCES

Adams, R.J. (1996). Metaphase spindles rotate in the neuroepithelium of rat cerebral cortex. J. Neurosci. *16*, 7610–7618.

Assmann, V., Jenkinson, D., Marshall, J.F., and Hart, I.R. (1999). The intracellular hyaluronan receptor RHAMM/IHABP interacts with microtubules and actin filaments. J. Cell Sci. *112*, 3943–3954.

Bond, J., Roberts, E., Mochida, G.H., Hampshire, D.J., Scott, S., Askham, J.M., Springell, K., Mahadevan, M., Crow, Y.J., Markham, A.F., et al. (2002). ASPM is a major determinant of cerebral cortical size. Nat. Genet. *32*, 316–320.

Bond, J., Roberts, E., Springell, K., Lizarraga, S.B., Scott, S., Higgins, J., Hampshire, D.J., Morrison, E.E., Leal, G.F., Silva, E.O., et al. (2005). A centrosomal mechanism involving CDK5RAP2 and CENPJ controls brain size. Nat. Genet. *37*, 353–355.

Butts, T., Green, M.J., and Wingate, R.J. (2014). Development of the cerebellum: simple steps to make a 'little brain'. Development *141*, 4031–4041.

Casini, P., Nardi, I., and Ori, M. (2010). RHAMM mRNA expression in proliferating and migrating cells of the developing central nervous system. Gene Expr. Patterns *10*, 93–97.

Chen, C.T., Hehnly, H., Yu, Q., Farkas, D., Zheng, G., Redick, S.D., Hung, H.F., Samtani, R., Jurczyk, A., Akbarian, S., et al. (2014). A unique set of centrosome proteins requires pericentrin for spindle-pole localization and spindle orientation. Curr. Biol. *24*, 2327–2334.

di Pietro, F., Echard, A., and Mroin, X. (2016). Regulation of mitotic spindle orientation: an integrated view. EMBO Rep. *17*, 1106–1130.

Dunsch, A.K., Hammond, D., Lloyd, J., Schermelleh, L., Gruneberg, U., and Barr, F.A. (2012). Dynein light chain 1 and a spindle-associated adaptor promote dynein asymmetry and spindle orientation. J. Cell Biol. *198*, 1039–1054.

Englund, C., Fink, A., Lau, C., Pham, D., Daza, R.A.M., Bulfone, A., Kowalczyk, T., and Hevner, R. (2005). Pax6, Tbr2, and Tbr1 are expressed sequentially by radial glia, intermediate progenitor cells, and postmitotic neurons in developing neocortex. J. Neurosci. *25*, 247–251.

Falk, S., Bugeon, S., Ninkovic, J., Pilz, G.A., Postiglione, M.P., Cremer, H., Knoblich, J.A., and Götz, M. (2017). Time-specific effects of spindle positioning on embryonic progeny pool composition and adult neural stem cell seeding. Neuron *93*, 777–791.

Fish, J.L., Kosodo, Y., Enard, W., Pääbo, S., and Huttner, W.B. (2006). Aspm specifically maintains symmetric proliferative divisions of neuroepithelial cells. Proc. Natl. Acad. Sci. USA *103*, 10438–10443.

Fujimori, A., Itoh, K., Goto, S., Hirakawa, H., Wang, B., Kokubo, T., Kito, S., Tsukamoto, S., and Fushiki, S. (2013). Disruption of Aspm causes microcephaly with abnormal neuronal differentiation. Brain Dev. *36*, 661–669.

Guernsey, D.L., Jiang, H., Hussin, J., Arnold, M., Bouyakdan, K., Perry, S., Babineau-Sturk, T., Beis, J., Dumas, N., Evans, S.C., et al. (2010). Mutations in centrosomal protein CEP152 in primary microcephaly families linked to MCPH4. Am. J. Hum. Genet. *87*, 40–51.

Groen, A.C., Cameron, L.A., Coughlin, M., Miyamoto, D.T., Mitchison, T.J., and Ohi, R. (2004). XRHAMM functions in Ran-dependent microtubule nucleation and pole formation during anastral spindle assembly. Curr. Biol. *14*, 1801–1811.

Gruber, R., Zhou, Z., Sukchev, M., Joerss, T., Frappart, P.O., and Wang, Z.Q. (2011). MCPH1 regulates the neuroprogenitor division mode by coupling the centrosomal cycle with mitotic entry through the Chk1-Cdc25 pathway. Nat. Cell Biol. *25*, 1325–1334.

Haldipur, P., Sivaprakasam, I., Periasamy, V., Govindan, S., and Mani, S. (2015). Asymmetric cell division of granule neuron progenitors in the external granule layer of the mouse cerebellum. Biol. Open *4*, 865–872.

Insolera, R., Bazzi, H., Shao, W., Anderson, K.V., and Shi, S.H. (2014). Cortical neurogenesis in the absence of centrioles. Nat. Neurosci. *17*, 1528–1535.

Jackson, A.P., Eastwood, H., Bell, S.M., Adu, J., Toomes, C., Carr, I.M., Roberts, E., Hampshire, D.J., Crow, Y.J., Mighell, A.J., et al. (2002). Identification of microcephalin, a protein implicated in determining the size of the human brain. Am. J. Hum. Genet. *71*, 136–142.

Joukov, V., Groen, A.C., Prokhorova, T., Gerson, R., White, E., Rodriguez, A., Walter, J.C., and Livingston, D.M. (2006). The BRCA1/BARD1 heterodimer modulates ran-dependent mitotic spindle assembly. Cell *127*, 539–552.

Konno, D., Shioi, G., Shitamukai, A., Mori, A., Kiyonari, H., Miyata, T., and Matsuzaki, F. (2008). Neuroepithelial progenitors undergo

LGN-dependent planar divisions to maintain self-renewability during mammalian neurogenesis. Nat. Cell Biol. *10*, 93–101.

Kotak, S., Busso, C., and Gönczy, P. (2012). Cortical dynein is critical for proper spindle positioning in human cells. J. Cell Biol. *199*, 97–110.

Li, H., Moll, J., Winkler, A., Frappart, L., Brunet, S., Hamann, J., Kroll, T., Verlhac, M.H., Heuer, H., Herrlich, P., et al. (2015). RHAMM deficiency disrupts folliculogenesis resulting in female hypofertility. Biol. Open *4*, 562–571.

Li, H., Frappart, L., Moll, J., Winkler, A., Kroll, T., Hamann, J., Kufferath, I., Groth, M., Taudien, S., Schütte, M., et al. (2016). Impaired planar cell division in the testis, caused by dissociation of RHAMM from the spindle, results in hypofertility and seminoma. Cancer Res. *76*, 6382–6395.

Maxwell, C.A., Keats, J.J., Crainie, M., Sun, X., Yen, T., Shibuya, E., Hendzel, M., Chan, G., and Pilarski, L.M. (2003). RHAMM is a centrosomal protein that interacts with dynein and maintains spindle pole stability. Mol. Biol. Cell *14*, 2262–2276.

Neumann, B., Walter, T., Hériché, J.K., Bulkescher, J., Erfle, H., Conrad, C., Rogers, P., Poser, I., Held, M., Liebel, U., et al. (2010). Phenotypic profiling of the human genome by time-lapse microscopy reveals cell division genes. Nature *464*, 721–727.

Noatynska, A., Gotta, M., and Meraldi, P. (2012). Mitotic spindle (DIS)orientation and DISease: cause or consequence? J. Cell Biol. *199*, 1025–1035.

Noctor, S.C., Martinez-Cerdeno, V., and Kriegstein, A.R. (2008). Distinct behaviors of neural stem and progenitor cells underlie cortical neurogenesis. J. Comp. Neurol. *508*, 28–44.

Peyre, E., and Morin, X. (2012). An oblique view on the role of spindle orientation in vertebrate neurogenesis. Dev. Growth Differ. *54*, 287.

Postiglione, M.P., Jüschke, C., Xie, Y., Haas, G.A., Charalambous, C., and Knoblich, J.A. (2011). Mouse inscuteable induces apical-basal spindle orientation to facilitate intermediate progenitor generation in the developing neocortex. Neuron *72*, 269–284.

Siller, K.H., and Doe, C.Q. (2009). Spindle orientation during asymmetric cell division. Nat. Cell Biol. *11*, 365–374.

Sohr, S., and Engeland, K. (2008). RHAMM is differentially expressed in the cell cycle and downregulated by the tumor suppressor p53. Cell Cycle *7*, 3448–3460.

Sun, T., and Hevner, R.F. (2014). Growth and folding of the mammalian cerebral cortex: from molecules to malformations. Nat. Rev. Neurosci. *15*, 217–232.

Tolg, C., Poon, R., Fodde, R., Turley, E.A., and Alman, B.A. (2003). Genetic deletion of receptor for hyaluronan-mediated motility (Rhamm) attenuates the formation of aggressive fibromatosis (desmoid tumor). Oncogene *22*, 6873–6882.

Williams, S.E., Garcia, I., Crowther, A.J., Li, S., Stewart, A., Liu, H., Lough, K.J., O'Neill, S., Veleta, K., Oyarzabal, E.A., et al. (2015). Aspm sustains postnatal cerebellar neurogenesis and medulloblastoma growth in mice. Development *142*, 3921–3932.

Woodworth, M.B., Custo Greig, L., Kriegstein, A.R., and Macklis, J.D. (2012). SnapShot: cortical development. Cell *151*, 918–918.e1.

Xie, Y., Jüschke, C., Esk, C., Hirotsune, S., and Knoblich, J. (2013). The phosphatase PP4c controls spindle orientation to maintain proliferative symmetric cell divisions in the developing neocortex. Neuron *79*, 254–265.

Yingli, J., Youn, Y.H., Darling, D., Toyo-oka, K., Pramparo, T., Hirotsune, S., and Wynshar-Boris, A. (2008). Neuroepithelial stem cell proliferation requires LIS1 for precise spindle orientation and symmetric division. Cell *132*, 474–486.

Zagon, I.S., and McLaughlin, P.J. (1987). The location and orientation of mitotic figures during histogenesis of the rat cerebellar cortex. Brain Res. Bull. *18*, 325–336.